Repurposing dasatinib for diffuse large B cell lymphoma

Claudio Scuoppo[a,b,1], Jiguang Wang[c,2], Mirjana Persaud[a], Sandeep K. Mittan[a], Katia Basso[a,b], Laura Pasqualucci[a,b], Raul Rabadan[c], Giorgio Inghirami[d], Carla Grandori[e], Francesc Bosch[a,f], and Riccardo Dalla-Favera[a,b,g,h,1]

[a]Institute for Cancer Genetics, Columbia University, New York, NY 10032; [b]Department of Pathology and Cell Biology, Columbia University, New York, NY 10032; [c]Department of Systems Biology, Columbia University, New York, NY 10032; [d]Department of Pathology and Laboratory Medicine, Weill Cornell Medical College, New York, NY 10065; [e]Cure First and SEngine Precision Medicine, Seattle, WA 98109; [f]Department of Hematology and Vall d'Hebron Institute of Oncology, University Hospital Vall d'Hebron, 08035 Barcelona, Spain; [g]Department of Genetics and Development, Columbia University, New York, NY 10032; and [h]Department of Microbiology and Immunology, Columbia University, New York, NY 10032

Contributed by Riccardo Dalla-Favera, June 26, 2019 (sent for review April 2, 2019; reviewed by Margaret A. Shipp and Wyndham H. Wilson)

To repurpose compounds for diffuse large B cell lymphoma (DLBCL), we screened a library of drugs and other targeted compounds approved by the US Food and Drug Administration on 9 cell lines and validated the results on a panel of 32 genetically characterized DLBCL cell lines. Dasatinib, a multikinase inhibitor, was effective against 50% of DLBCL cell lines, as well as against in vivo xenografts. Dasatinib was more broadly active than the Bruton kinase inhibitor ibrutinib and overcame ibrutinib resistance. Tumors exhibiting dasatinib resistance were commonly characterized by activation of the PI3K pathway and loss of PTEN expression as a specific biomarker. PI3K suppression by mTORC2 inhibition synergized with dasatinib and abolished resistance in vitro and in vivo. These results provide a proof of concept for the repurposing approach in DLBCL, and point to dasatinib as an attractive strategy for further clinical development in lymphomas.

dasatinib | DLBCL | PTEN

Diffuse large B cell lymphoma (DLBCL) is the most frequent B cell non-Hodgkin lymphoma, accounting for 22,000 new cases per year in the United States. The current first-line therapeutic approach involves the combination of an anthracycline-based regimen with CD20-targeted antibodies [cyclophosphamide, doxorubicin, vincristine, and prednisone plus rituximab (R-CHOP)] and is curative in 60% of cases (1), with better outcome for the germinal center B cell-like (GCB), than the activated B cell-like (ABC) subtype (2). Patients who fail to respond to R-CHOP usually are resistant to other chemotherapies and have a dismal prognosis. As a consequence, a number of targeted drugs have been developed for DLBCL, including the irreversible Bruton tyrosine kinase (BTK) inhibitor ibrutinib (3), which has been shown to be active against a subset of ABC-DLBCLs carrying *CD79A/B* gene mutations (4). However, resistance to ibrutinib has been observed, and in indolent B-NHLs, it is commonly driven by mutations involving the BTK 481 cysteine, the residue binding to ibrutinib (5).

Inhibitors of the phosphatidylinositol-3-kinase (PI3K) pathway have also emerged as an important class of therapeutic agents in DLBCL (6). PI3K signaling is the sole requirement for BCR-dependent survival signals in normal germinal center B cells (7) and in a subset of DLBCLs (8). In addition, inactivating mutations and copy loss of phosphatase and tensin homolog deleted on chromosome 10 (PTEN) (9), whose enzymatic activity counteracts PI3K, are frequently found in a subset of GCB-DLBCLs. However, the scope and benefit of PI3K-targeted therapy is still limited to a subset of patients with DLBCL (10).

Overall, the incomplete success in curing DLBCL underscores the need for additional efforts to identify novel compounds active in this disease. Toward this end, we reasoned that the hundreds of drugs and targeted compounds approved by the US Food and Drug Administration and in various stages of clinical development represent a very rich armamentarium of drugs that may include some capable of targeting known or novel pathway dependencies in DLBCL. Therefore, testing these drugs for efficacy in DLBCL may reveal new pathogenetic mechanisms in this disease and, in addition, would make them readily testable in the clinical setting without the long time and significant resources involved in de novo drug development.

Here we report that a DLBCL-directed repurposing effort, involving a large number of drugs and other targeted compounds approved by the US Food and Drug Administration, has led to the identification of the multikinase inhibitor dasatinib as active in a major subset of DLBCLs. In particular, we show that dasatinib, which is in clinical use for the treatment of chronic myelogenous leukemia (11), is active against 50% of DLBCLs and acts independent of BTK in ABC-DLBCL. In addition, using in vitro and in vivo preclinical evidence, we identify the mechanism and a biomarker associated with dasatinib resistance, as well as a combinatorial regimen that can revert it.

Results

Screen for Repositioning Compounds Identifies Dasatinib as the Lead DLBCL-Active Drug. To identify compounds of potential value for repurposing in DLBCL, we screened 2 libraries including a total of 2,160 compounds representative of drugs approved for clinical use in the United States, Japan, and Europe; natural products; and targeted compounds at various stages of clinical testing. Using an ATP-based assay (12), we first high-throughput tested these compounds for their ability to suppress GCB-DLBCL (n = 3),

Significance

Novel therapies are needed for ~40% of patients with diffuse large B cell lymphoma (DLBCL) who do not respond to standard immunochemotherapy. Here we show that dasatinib, a drug used in B cell acute lymphoblastic leukemia and chronic myelogenous leukemia, may be repositioned for DLBCL therapy and combined with mTORC2 inhibitors for resistant cases. Our results can provide the basis for clinical trials using dasatinib for DLBCL as well as other lymphoid malignancies, which depend on cellular pathways targeted by dasatinib.

Author contributions: C.S. and R.D.-F. designed research; C.S., M.P., S.K.M., and C.G. performed research; C.S., J.W., K.B., L.P., R.R., G.I., C.G., and F.B. contributed new reagents/analytic tools; C.S., J.W., and R.D.-F. analyzed data; and C.S. and R.D.-F. wrote the paper.

Reviewers: M.A.S., Dana-Farber Cancer Institute; and W.H.W., NIH.

Conflict of interest statement: G.I. and reviewer Margaret Shipp are coauthors on a 2016 paper.

[1]To whom correspondence may be addressed. Email: cs3064@cumc.columbia.edu or rd10@cumc.columbia.edu.

[2]Present address: Division of Life Science and Department of Chemical and Biological Engineering, Hong Kong University of Science and Technology.

This article contains supporting information online at www.pnas.org/lookup/suppl/doi:10.1073/pnas.1905239116/-/DCSupplemental.

Published online August 5, 2019.

ABC-DLBCL ($n = 3$), or mantle cell lymphoma (MCL; $n = 3$) cell lines, focusing on disease-specific activities as an indication of pathway specificity and lack of general toxicity. Compounds that were active against at least 1 cell line (~14%) were subsequently validated in a secondary screen across a 4-concentration log range (0.01–10 μM). We defined for each compound and cell line a sensitivity area by fitting 5-point logistic curves to the response data and calculating the area complementary to the area under the curve of the dose–response function (13) (*SI Appendix*, *Materials and Methods*). We then generated a sensitivity plot in which the position of each drug indicates the relative effect for each of the 3 subtypes (*SI Appendix*, Fig. S1 and Table S1).

This screen identified the Src/Abl tyrosine kinase inhibitor dasatinib as the most potent and specific compound in DLBCL (Fig. 1*A*). Dasatinib displayed activity in 5 of 6 DLBCL lines, with no preferential activity in GCB versus ABC subtypes and no significant activity against MCL cell lines (Fig. 1*B*). Of note, other 8 multikinase inhibitors included in the screen were poorly effective or nonspecific (Fig. 1*A*), suggesting that the activity of dasatinib is not due to global suppression of tyrosine phosphorylation.

These results were confirmed in a larger panel of 32 DLBCL lines, showing that dasatinib is toxic to a significant subset of DLBCL lines, regardless of subtype. Specifically, 48% (11 of 23) GCB-DLBCL and 56% (5 of 9) ABC-DLBCL cell lines were found to be sensitive to dasatinib, using a sensitivity threshold corresponding to a 125-nM IC50 (14) (Fig. 1*C*). Notably, dasatinib was active also in vivo, as it suppressed the growth of xenografts, as assessed by luciferase imaging and tumor volume measurements in the luciferized HBL1 and WSU-NHL DLBCL cell lines with no overt toxicity at a dose previously used in several preclinical models of Bcr-Abl-driven leukemias (15–17) (Fig. 2 and *SI Appendix*, Fig. S2). These results provide preclinical evidence of the activity of dasatinib against a large subset of DLBCL cases representative of both subtypes of this disease.

Dasatinib Activity Is Independent of BTK and Overcomes BTK Resistance in DLBCL. Since the dasatinib inhibition profile includes BTK, a key signal transducer in the BCR chronically active ABC-DLBCL subtype and the target of the drug ibrutinib (4), we investigated whether dasatinib and ibrutinib activities overlap in DLBCL. We compared the responses of the 32-cell line panel to both drugs, using sensitivity areas generated from dosage-dependent responses as described earlier, and used a sensitivity threshold for ibrutinib corresponding to a 87 nM IC50 (18). We identified 3 groups of response: a subset comparably sensitive to ibrutinib and dasatinib, which includes the 3 cell lines carrying *CD79A/B* mutations (LY10, TMD8, HBL1); a second cluster including DLBCL lines significantly more sensitive to dasatinib than ibrutinib; and a third cluster comprising lines resistant to both drugs (Fig. 3*A*). These data indicate that dasatinib has a range of activity broader than ibrutinib, and preliminarily suggested that dasatinib activity is not restricted by BTK inhibition alone.

To directly test the role of BTK in dasatinib sensitivity, we took advantage of the BTK C481S mutant, which confers ibrutinib resistance by impairing ibrutinib binding. We transduced LY10, TMD8, and HBL1 cells (CD79A/B mutant ABC-DLBCLs) with vectors encoding wild-type BTK (BTK WT) or C481S mutant BTK (BTK C481S) or empty vector as control (EV). As expected, BTK C481S conferred resistance to ibrutinib, while BTK WT did not. In contrast, dasatinib was equally effective against BTK WT and C481S cells. (Fig. 3 *B–D*). These results were confirmed in vivo (*SI Appendix*, Fig. S3).

To understand whether dasatinib is effective in suppressing the activation of BTK C481S, we tested the auto-phosphorylation of BTK WT and C481S at tyrosine 223 after treatment with dasatinib or ibrutinib (15 nM). As expected, phosphorylation of BTK WT, but not BTK-C481S, was suppressed by ibrutinib. However, dasatinib was equally ineffective in suppressing BTK-C481S autophosphorylation

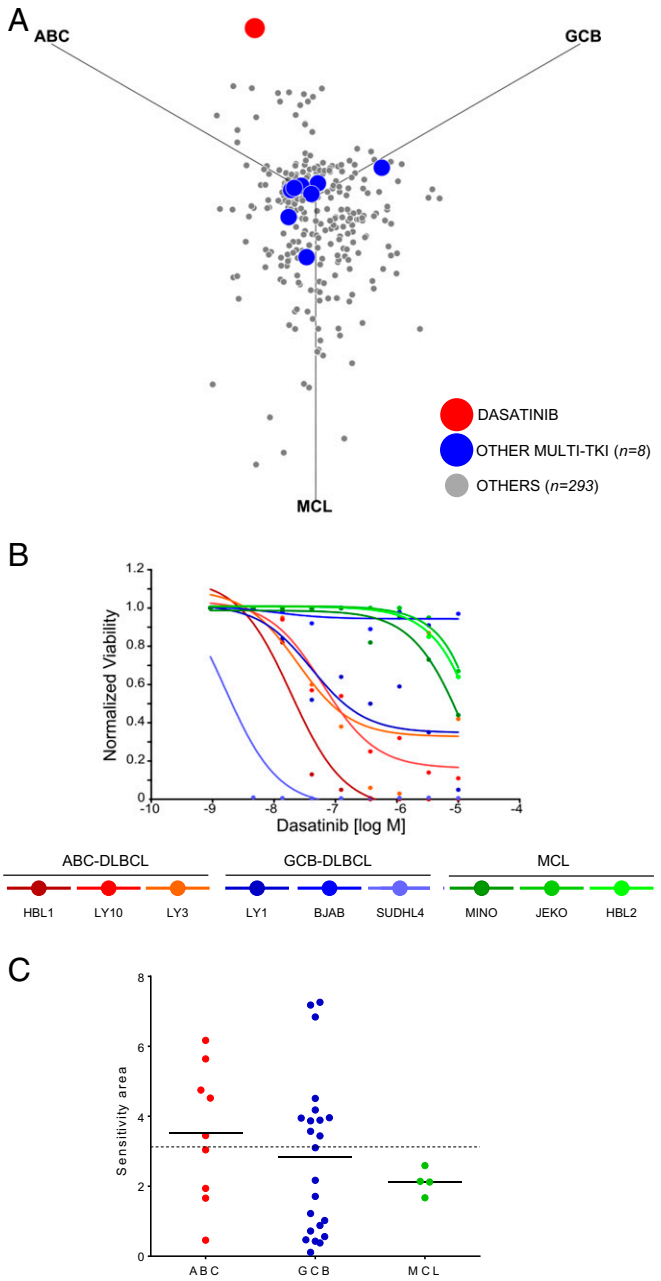

Fig. 1. A screen for repositioning compounds identifies dasatinib as the lead DLBCL-specific agent. (*A*) Specificity plot of 302 compounds tested for activity in ABC-DLBCL, GCB-DLBCL, and MCL lines ($n = 3$, each). Dasatinib, red; other multikinase inhibitors are indicated in blue ($n = 8$; dovitinib, lenvatinib, masitinib, nilotinib, ponatinib, saracatinib, sunitinib, and tandutinib). (*B*) Dose–response curves to dasatinib of ABC-DLBCL, GCB-DLBCL, and MCL ($n = 3$ each). (*C*) Distribution of dasatinib sensitivity in ABC- (red; $n = 9$) or non-ABC DLBCL (GCB, blue; $n = 23$) and MCL (green; $n = 4$) lines. Horizontal lines represent averages. Dotted line represents sensitivity threshold for dasatinib (3.125).

(Fig. 3 *E–G*). Taken together, these results indicate that the activity of dasatinib in suppressing DLBCL line growth is independent from BTK activity and mutational status, and provide preclinical evidence for the use of dasatinib against ibrutinib-resistant tumors (*Discussion*).

FYN as a Major Dasatinib Target in DLBCL. Since the above results suggest that dasatinib may act through non-BTK targets, we

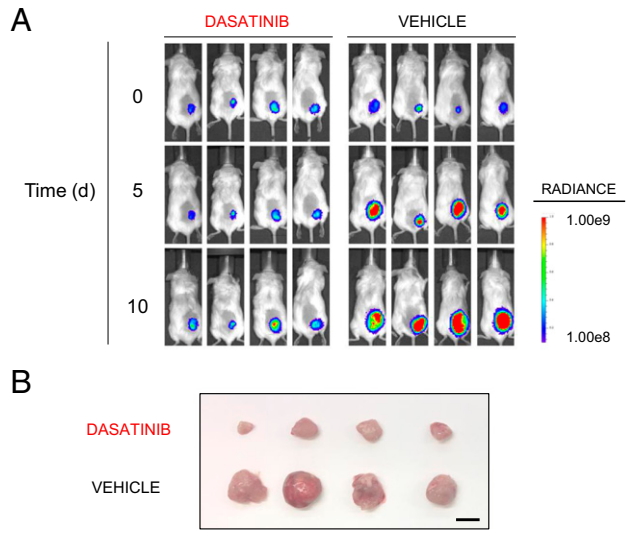

Fig. 2. Dasatinib suppresses DLBCL growth in vivo. (*A*) Luciferase imaging of NOD/SCID mice s.c. transplanted with HBL1 cells carrying a Luciferase Tomato expressing vector (HBL1 LTS) and treated with dasatinib (10 mg/kg twice daily) or vehicle only ($n = 4$/group). (*B*) Resection of s.c. tumors from mice treated with dasatinib or vehicle at day 10. Magnification bar, 10 mm. Fold change of diameter (*C* and *D*) and flux over time, relative to time 0, for dasatinib-treated (red) or vehicle only (black) HBL1-LTS xenotransplants. Error bars represent SDs (***$P < 0.001$, *t* test; $n = 8$ mice per group). Statistics refer to day 10 measurements.

examined its activity against members of the family of Src/Abl family kinases (SFKs), which are known to be inhibited by dasatinib. In particular, we examined the 3 SFKs (LYN, FYN, and BLK) that are associated with proximal BCR signaling, as shown by CD79A/B coimmunoprecipitation approaches (19). To test which SFK needs to be suppressed for dasatinib to exert its action, we took advantage of gatekeeper mutants (GK) of each SFK. The GK residue is important for binding of type I/II TK inhibitors to the target kinase, and its mutation confers resistance by decreasing accessibility to the inhibitor (20, 21). We then transduced dasatinib-sensitive DLBCL cell lines (HBL1: ABC-DLBCL, *CD79*-mutated; and WSU-NHL: GCB-DLBCL, *CD79*-wild type) with WT or GK cDNAs for each of the 3 SFKs, alone or in combination, and tested their ability to induce resistance to dasatinib. This experiment revealed that when expressed alone, FYN GK was the most effective in inducing dasatinib resistance, both in HBL1 and in WSU-NHL cells. In ABC-DLBCL cells, FYN GK-induced resistance was further increased by the presence of LYN or BLK GK, while the combination of the 3 GK together did not confer further resistance in both cell lines (Fig. 4).

PTEN Loss and PI3K Activation as Biomarkers of Dasatinib Resistance. To dissect the mechanisms of dasatinib resistance, we searched for correlations between specific genetic lesions found in the cell line panel and dasatinib sensitivity. We initially identified PTEN loss by inactivating mutations and/or deletions as the top candidate feature of resistant cells, being detectable in 25% (4 of 16) resistant lines (Fig. 5 *A* and *B*). In addition, PTEN protein was undetectable by Western blot analysis in 5 additional resistant lines that do not harbor PTEN genetic alterations, suggesting that PTEN is also targeted by epigenetic mechanisms (22) (Fig. 5*B*). Overall, 56% (9 of 16) of the resistant lines showed PTEN protein loss compared with 13% (2 of 16; $P = 0.02$) of the sensitive cell lines (Fig. 5*C*).

PTEN inactivation was matched by AKT S473 phosphorylation (Fig. 5*B*), which was easily detected in all PTEN-null DLBCLs and in 2 additional resistant lines (DB, SUDHL10). As sensitive cell lines also show residual AKT phosphorylation, we asked whether dasatinib activity was dependent on its ability to suppress AKT phosphorylation, and was prevented by the absence of PTEN-mediated negative regulation. We treated all AKT-positive resistant cell lines ($n = 11$), as well as 6 sensitive cell lines, with 2 different doses of dasatinib (1 and 10 nM), and

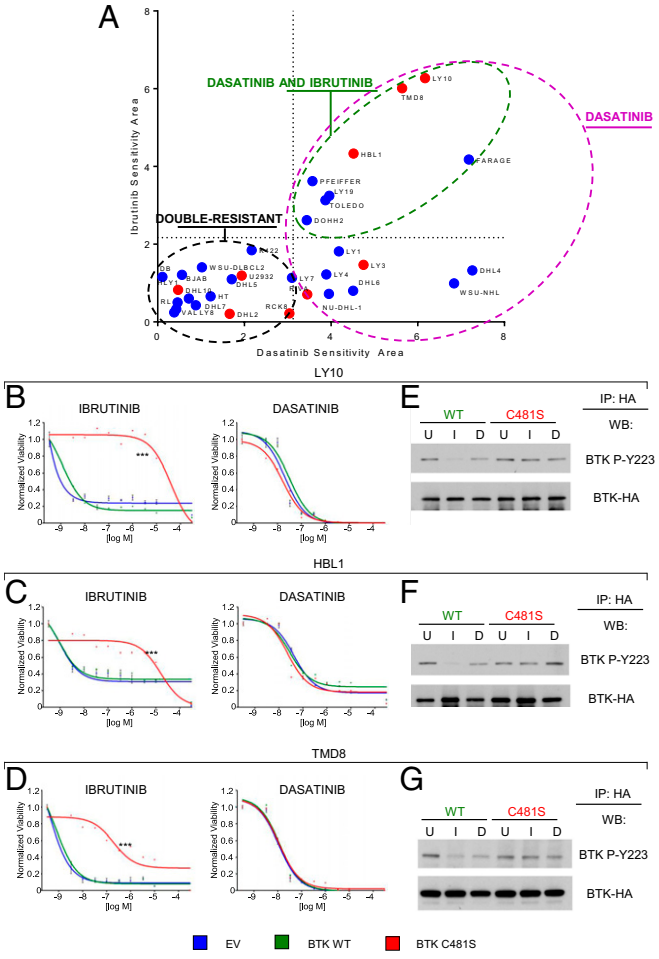

Fig. 3. Dasatinib overcomes ibrutinib resistance resulting from the C481S BTK mutation and acts independent of BTK. (*A*) Sensitivity plot of ibrutinib (*y* axis) and dasatinib (x-axis) across 32 DLBCL lines (GCB, blue; ABC, red; FARAGE, DLBCL/PMBL) classified as dasatinib-sensitive ($n = 16$, violet circle), equivalently sensitive to dasatinib and ibrutinib ($n = 8$, green circle), and resistant to both drugs ($n = 16$, black circle). Dotted lines represent sensitivity thresholds: dasatinib, 3.125; ibrutinib, 2.169. (*B*) Dose–response curves to ibrutinib (*Left*) and dasatinib (*Right*) for LY10, (*C*) HBL1, and (*D*) TMD8 cells transduced with empty vector (EV, blue) or vectors encoding WT BTK (BTK WT, green) or ibrutinib-resistant mutant BTK (BTK C481S, red; ***$P < 0.001$). (*E*) Western blot of HA immunoprecipitates for phospho BTK-Y223, BTK-WT, and BTK-C481S in LY10, (*F*) HBL1, and (*G*) TMD8 cells treated with 15 nM ibrutinib (I) or dasatinib (D) or DMSO only (U, untreated) for 1 h.

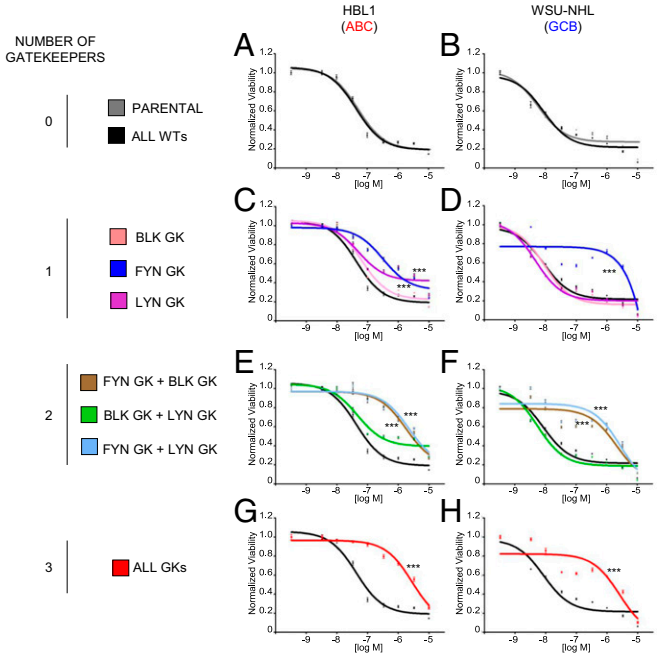

Fig. 4. Suppression of FYN is indispensable for dasatinib activity. Dose–response curves to dasatinib for HBL1 (*A, C, E, G*) and WSU-NHL (*B, D, F, H*) cells engineered to express BLK, FYN, or LYN either WT or GK in each of the possible 8 combinations (***$P < 0.001$; *t* test). For each combination, the indicated gatekeeper cDNA(s) was cotransduced with the remaining WT kinase(s). Error bars represent SDs ($n = 4$ replicates per dose–response point). Statistical significance is shown for the indicated concentrations and gatekeeper combination vs. the ALL WT combination.

probed them for AKT S473 phosphorylation. One-hour dasatinib treatment abrogated AKT phosphorylation in all sensitive cell lines, while S473 phosphorylation persisted in PTEN-negative resistant lines (Fig. 6). Based on this data, we conclude that it is the PTEN-dependent inability to suppress AKT activity, rather than the level of AKT phosphorylation, that drives resistance to dasatinib.

Since PTEN is a negative regulator of the PI3K pathway, we directly tested whether activation of this pathway is responsible for the induction of dasatinib resistance. PTEN suppression by the inhibitor SF1670 induced a modest but significant increase in AKT S473 phosphorylation and dasatinib resistance in 2 dasatinib-sensitive lines (*SI Appendix*, Fig. S4). Since this modest effect of PTEN inactivation may be due to the need for additional PI3K activation to activate AKT, we directly tested the effect of PI3K activation by transducing 3 dasatinib-sensitive DLBCL lines (WSU-NHL, FARAGE, and HBL1) with vectors encoding either WT PIK3CA (PIK3CA WT) or a constitutively active PIK3CA mutant (PIK3CA H1047R), and tested these isogenically engineered cell lines for dasatinib sensitivity. The results showed that PIK3CA H1047R-expressing cells were significantly more resistant to dasatinib than PIK3CA WT cells (*SI Appendix*, Fig. S5 *A–C*, *Left*). Consistently, dasatinib treatment led to rapid suppression of AKT S473 phosphorylation in PI3KCA WT cells, while the same phosphorylation persisted in PIK3CA H1047R cells (*SI Appendix*, Fig. S5 *A–C*, *Middle* and *Right*). Treatment of xenotransplants of luciferized HBL1 cells expressing either PI3K WT or PI3K H1047R in NOD/SCID mice confirmed these results in vivo by showing that PI3K H1047R HBL1 tumors did not respond to dasatinib, as documented by luciferase imaging and tumor volume measurement (*SI Appendix*, Fig. S5 *D–G*). Finally, these results were confirmed in PDX-derived cultures, which showed that the PTEN-negative YLL did not respond to dasatinib, while other PTEN-positive ones did (*SI Appendix*, Fig. S6). Overall, these data indicate that activation of PI3K signaling induces resistance to dasatinib.

PI3K Inhibition by Targeting mTOR Synergizes with Dasatinib. These results led us to explore the potential of inhibitors of the PI3K/AKT/mTOR pathway for treating dasatinib-resistant DLBCLs. Thus, we first screened a set of compounds including PI3KCD/PI3KCG inhibitors [CAL-101 (23) and IPI-145 (24)], the AKT inhibitor MK-2206 (25), the mTORC1 inhibitor rapamycin (26), and mTOR kinase inhibitors [mTORK_i, OSI-027 (27) and INK-128 (28)] for their ability to suppress AKT activation in PTEN-negative, dasatinib-resistant cell lines ($n = 4$). We identified the mTORC inhibitor INK-128 as the most effective in suppressing AKT activation in all the cell lines tested (Fig. 7*A*). Consistent with suppression of AKT S473 phosphorylation, INK-128 was effective on all 9 PTEN-negative, dasatinib-resistant cell lines (*SI Appendix*, Fig. S7), as shown by dose-dependent response curves and phospho-S473 AKT immunoblots.

While these results support the use of mTOR inhibitors for dasatinib-resistant cases, their therapeutic use would be limited by the potential toxicities, which have been observed in preclinical practice when used as single agent (29). We thus explored whether dasatinib and INK-128 could synergize, and therefore be used at lower dosages, allowing for both reduced toxicity and suppression of dasatinib-resistant lymphomas. Consistent with this hypothesis, dasatinib and INK-128 showed synergic effect in 3 PTEN-negative dasatinib-resistant lines (Fig. 7*B*). Accordingly,

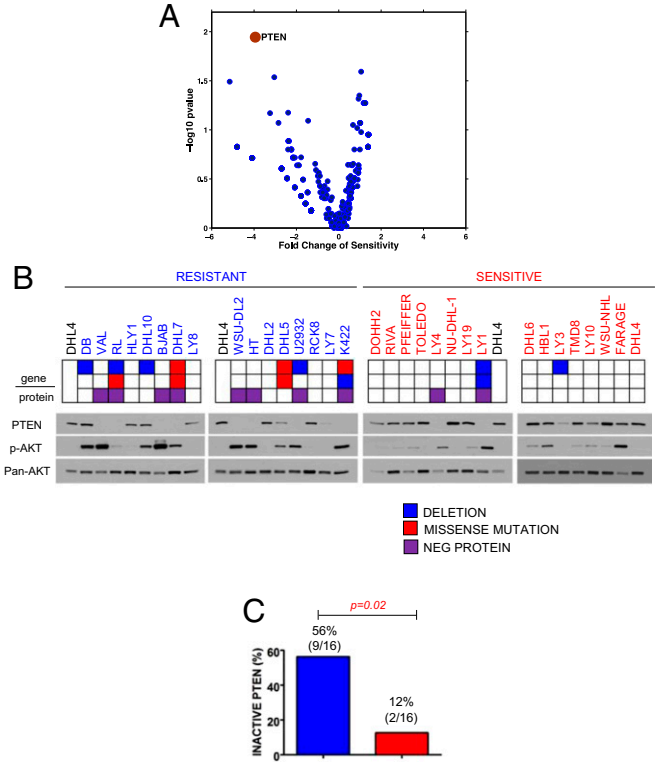

Fig. 5. PTEN loss is associated with dasatinib resistance. (*A*) Correlative measure of dasatinib resistance for the top 100 candidate sensitivity determinants (PTEN, red dot; other, blue dots). (*B*) PTEN, phospho-AKT S473, and pan-AKT detection by Western blot in dasatinib-resistant ($n = 16$, blue) and dasatinib-sensitive ($n = 16$, red) DLBCLs. Keys indicate PTEN status and related genetic lesions: deletions, blue; missense mutations, red; protein-negativity (in the absence of genetic lesions), violet. (*C*) Frequency of PTEN-inactivation in dasatinib-resistant ($n = 16$, blue) and dasatinib-sensitive cell lines ($n = 16$, red; $P = 0.02$, Fisher's exact test).

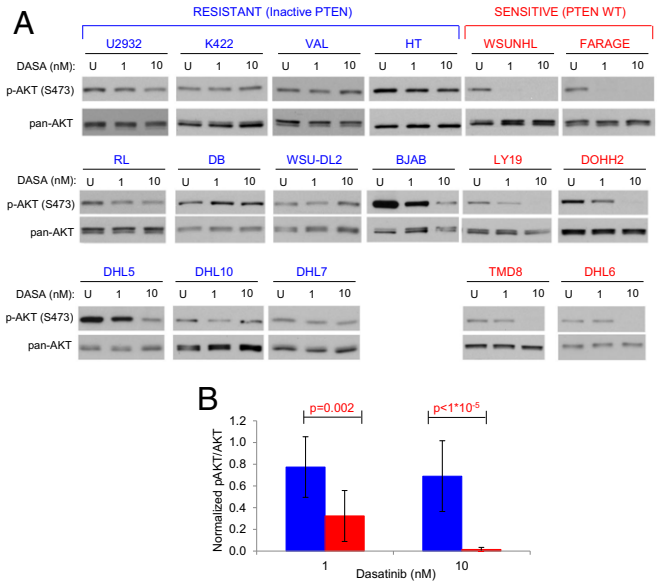

Fig. 6. PTEN loss results in dasatinib inability to restrict PI3K/AKT signaling. (*A*) Western blot analysis of phospho-S473 AKT for AKT-active, dasatinib-resistant (blue, $n = 11$) and dasatinib-sensitive (red, $n = 6$) lines, either untreated (U) or treated with 1 or 10 nM dasatinib. (*B*) Averages for AKT activation (pAKT/AKT ratio) in resistant (blue, $n = 11$) and sensitive (red, $n = 6$) lines on dasatinib treatment at the indicated concentrations. Error bars indicate SDs. *P* values indicate *t* test.

combinatorial treatment of dasatinib (10 mg/kg twice daily) and INK-128 (0.75 mg/kg 3 times a week) in vivo was effective in suppressing the growth of KARPAS 422 xenografts, as measured by luciferase imaging and tumor volume (Fig. 7 *C*–*F*). Finally, we detected a 3-fold progression-free survival benefit of the combined treatment compared with single or untreated controls (Fig. 7*G*). Overall, these results provide preclinical in vitro and in vivo evidence for the use of mTOR inhibitors/dasatinib combinatorial treatments in dasatinib-resistant DLBCL.

Discussion

Dasatinib has been previously examined for its potential activity against non-Hodgkin lymphoma in a phase 1/2 clinical trial including 33 patients with heterogeneous B- and T-NHL histologies (30). Although it showed a limited number of both partial and complete responses with acceptable toxicities, this study included only 8 DLBCLs and did not explore the status of PI3K/AKT/mTOR activation in these cases. These limitations, together with the preclinical results presented here, suggest that the clinical activity of dasatinib against DLBCL should be reexamined by addressing an informative series of patients and using the biomarkers of sensitivity and resistance shown here.

A second aspect of our study involves the potential use of dasatinib for cases resistant to BTK-targeting agents such as ibrutinib. A recent study has explored the preclinical activity of various multi-TK inhibitors and concluded that masitinib may be more effective than dasatinib against ibrutinib-resistant DLBCL (31). We note, however, that the authors defined resistance using micromolar concentration of ibrutinib in BCR-stimulated lymphomas irrespective of their subtype and genetics. In addition, masitinib was effective in DLBCL lines only at nonclinically relevant micromolar concentrations. Our study demonstrates that native, unstimulated DLBCL cell lines of defined genetic/epigenetic features can be killed by nanomolar, pharmacologically relevant concentrations. These observations, together with the fact that dasatinib is already approved for clinical use, point to this drug as a strong candidate for DLBCL treatment.

Although not directly addressed here, several observations suggest that dasatinib may be active against a significantly expanded spectrum of B cell malignancies. First, we show that dasatinib kills cells by a mechanism that is independent of BTK targeting, suggesting that this drug may act on B-NHLs that respond initially to ibrutinib but acquire resistance after mutation of BTK cysteine 481 (5). Accordingly, we preliminary show that a PDX derived from a patient with Richter syndrome treated with

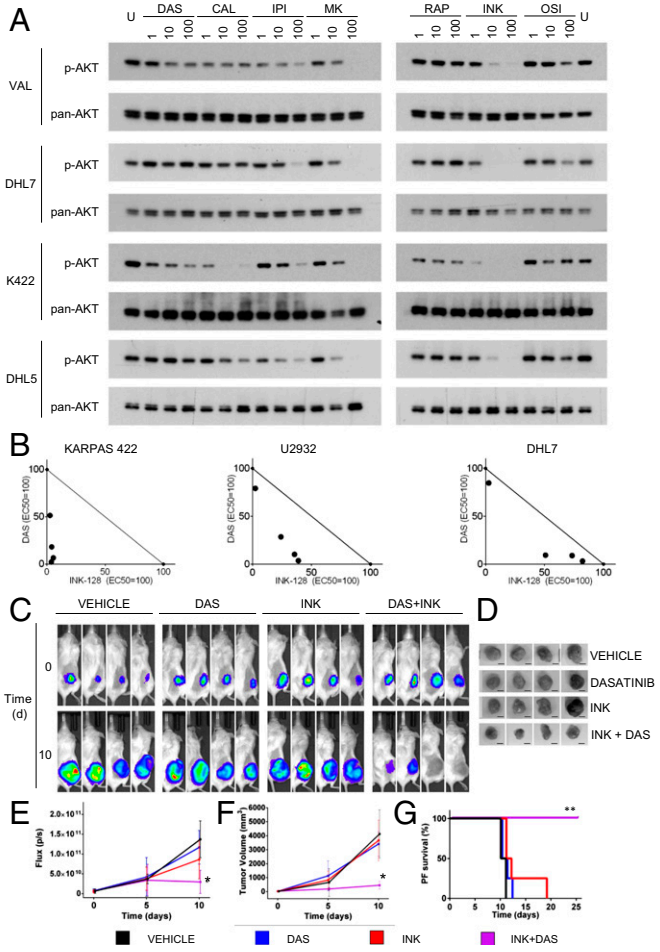

Fig. 7. mTORC inhibition synergizes with dasatinib in PTEN-negative DLBCLs. (*A*) Phospho-AKT S473 Western blot comparing the effect of PI3K pathway inhibitors on AKT activation in 4 dasatinib-resistant cell lines at the indicated concentration (nM; U, untreated). Inhibitors are indicated as follows: DAS, dasatinib; CAL, CAL-101; IPI, IPI-145; MK, MK-2206; RAPA, rapamycin; OSI, OSI-027; INK, INK-128. Pan-AKT was used for normalization. (*B*) Isobolograms for dasatinib-resistant, PTEN-disrupted lines ($n = 3$) for combinatorial effect between dasatinib and INK-128. EC_{50} values for each drug were used to define a normalized concentration set to 100. The diagonal line joining the 2 EC_{50} represents the line of additivity. Each dot represents a combinatorial IC50 concentration. Synergy is identified by dots below the additivity line ($n = 4$ per assay). (*C*) Luciferase imaging of NOD/SCID mice transplanted s.c. with dasatinib-resistant Karpas 422 cells carrying a Luciferase Tomato expressing vector and treated with dasatinib (10 mg/kg twice daily), INK-128 (0.75 mg/kg 3 times/week), dasatinib, and INK-128 in combination or vehicle only. (*D*) Resection of s.c. tumors in the cohorts described above at day 10 ($n = 4$ each). Bar, 10 mm. (*E*) Measurements of flux and (*F*) tumor volume over time relative to time 0 in mice treated with vehicle only (black), dasatinib (red), INK-128 (blue), or dasatinib in combination with Ink-128 (violet). Error bars represent SDs (*$P < 0.05$, *t* test; $n = 8$ mice per group). (*G*) Progression-free survival (defined as diameter smaller than 20 mm) of NOD-SCID mice transplanted s.c. with luciferized KARPAS-422 lymphoma cells and treated as indicated (**$P < 0.01$; log-rank test).

ibrutinib and evolved into ibrutinib resistance in vivo responded to dasatinib in ex vivo cultures (*SI Appendix*, Fig. S6). Second, the spectrum of malignant conditions that carry ibrutinib-sensitive genetics is rapidly expanding, and now includes chronic lymphocytic leukemia, Waldenstrom macroglobulinemia, and 75% of primary central nervous system lymphomas (32). In all these diseases, dasatinib could serve as a first-line or as a second-line treatment option in the event of acquired ibrutinib resistance.

The mechanism by which dasatinib kills DLBCL cells remains partially unknown. Previous work has reported that dasatinib decreases the phosphorylation of several molecules including IκB-alpha, AKT, ERK, and LYN (4). Our results clearly show a central role for AKT targeting, but also point to FYN as a major target, whose activity in response to dasatinib cannot be surrogated by LYN. This apparently contrasting observation may be explained by the fact that previous conclusions were based on loss-of-function approaches (33). Conversely, our approach involves the use of dasatinib-resistant (gatekeeper) mutations and may be more effective in identifying the molecules that are more prominent in sustaining BCR signaling and determining dasatinib activity. Overall, additional studies are needed to comprehensively identify the key targets of dasatinib activity, since the results could have important implications for the clinical use of this drug.

Despite its broad spectrum of activity, which includes ABC-DLBCL as well as a fraction of GCB-DLBCL, a subset of cases remains resistant to dasatinib. We identify loss of PTEN expression due to genetic or epigenetic mechanisms as a predictor of dasatinib resistance in 55% of resistant cell lines tested. Consistently, PTEN suppression (*SI Appendix*, Fig. S4) and PI3K activation induced resistance to dasatinib (*SI Appendix*, Fig. S5), indicating that the balance between PI3K and PTEN activities determines dasatinib sensitivity. This conclusion prompted the testing of several inhibitors of the PI3K pathway as potential partners that could eliminate dasatinib resistance. Our results show that mTOR inhibitors, such as INK-128, can counteract deregulated PI3K activity more efficiently than direct gamma/delta-specific PI3K or AKT inhibitors because of the ability of mTOR inhibitors to suppress mTOR-mediated AKT activation and, most likely, because AKT activation is more directly controlled by mTOR than by PI3K in these cells. Of note, pan-PI3K inhibitors have been shown to be effective in B-NHLs (10, 34) and may offer alternative venues to interfere with deregulated PI3K activity in PTEN-negative DLBCLs. A relevant aspect of the INK-128/dasatinib combination is their clear synergistic effect, which suggests its potential clinical use at lower doses, thus alleviating the toxicities that have been reported for dasatinib and especially for mTOR inhibitors (35).

Materials and Methods

Detailed methods for drug screens, drug specificity assessment, identification of predictors of resistance, dose–response assays, combinatorial studies, cell lines, lentivirus production, Western blot assays, animal studies, and statistical analysis are available in the *SI Appendix*.

ACKNOWLEDGMENTS. We thank the members of the R.D.-F. and R.R. laboratories for helpful discussions. This research was funded in part through the National Institutes of Health/National Cancer Institute Cancer Center Support Grant P30CA013696 and used the Flow Core and Transgenic Mouse facilities. C.S. was supported by a Leukemia Lymphoma Society Career Development Program (CDP) fellowship and by a Career Enhancement Program (CEP) fellowship funded by grant NIH SPORE P50CA192937. R.D.-F. is supported by grant NIH R35CA210105. R.R. was supported by grant NIH U54CA193313-01.

1. M. J. Maurer *et al*., Diagnosis-to-treatment interval is an important clinical factor in newly diagnosed diffuse large B-cell lymphoma and has implication for bias in clinical trials. *J. Clin. Oncol.* **36**, 1603–1610 (2018).
2. A. A. Alizadeh *et al*., Distinct types of diffuse large B-cell lymphoma identified by gene expression profiling. *Nature* **403**, 503–511 (2000).
3. L. A. Honigberg *et al*., The Bruton tyrosine kinase inhibitor PCI-32765 blocks B-cell activation and is efficacious in models of autoimmune disease and B-cell malignancy. *Proc. Natl. Acad. Sci. U.S.A.* **107**, 13075–13080 (2010).
4. R. E. Davis *et al*., Chronic active B-cell-receptor signalling in diffuse large B-cell lymphoma. *Nature* **463**, 88–92 (2010).
5. J. A. Woyach *et al*., Resistance mechanisms for the Bruton's tyrosine kinase inhibitor ibrutinib. *N. Engl. J. Med.* **370**, 2286–2294 (2014).
6. C. L. Batlevi, A. Younes, Revival of PI3K inhibitors in non-Hodgkin's lymphoma. *Ann. Oncol.* **28**, 2047–2049 (2017).
7. L. Srinivasan *et al*., PI3 kinase signals BCR-dependent mature B cell survival. *Cell* **139**, 573–586 (2009).
8. L. Chen *et al*., SYK inhibition modulates distinct PI3K/AKT- dependent survival pathways and cholesterol biosynthesis in diffuse large B cell lymphomas. *Cancer Cell* **23**, 826–838 (2013).
9. B. Chapuy *et al*., Molecular subtypes of diffuse large B cell lymphoma are associated with distinct pathogenic mechanisms and outcomes. *Nat. Med.* **24**, 679–690 (2018).
10. K. Bojarczuk *et al*., Targeted inhibition of PI3Kα/δ is synergistic with BCL-2 blockade in genetically defined subtypes of DLBCL. *Blood* **133**, 70–80 (2019).
11. N. P. Shah *et al*., Overriding imatinib resistance with a novel ABL kinase inhibitor. *Science* **305**, 399–401 (2004).
12. S. P. Crouch, R. Kozlowski, K. J. Slater, J. Fletcher, The use of ATP bioluminescence as a measure of cell proliferation and cytotoxicity. *J. Immunol. Methods* **160**, 81–88 (1993).
13. J. Barretina *et al*., The cancer cell line encyclopedia enables predictive modelling of anticancer drug sensitivity. *Nature* **483**, 603–607 (2012).
14. C. Yang *et al*., Tyrosine kinase inhibition in diffuse large B-cell lymphoma: Molecular basis for antitumor activity and drug resistance of dasatinib. *Leukemia* **22**, 1755–1766 (2008).
15. N. Boulos *et al*., Chemotherapeutic agents circumvent emergence of dasatinib-resistant BCR-ABL kinase mutations in a precise mouse model of Philadelphia chromosome-positive acute lymphoblastic leukemia. *Blood* **117**, 3585–3595 (2011).
16. Y. Hu *et al*., Targeting multiple kinase pathways in leukemic progenitors and stem cells is essential for improved treatment of Ph+ leukemia in mice. *Proc. Natl. Acad. Sci. U.S.A.* **103**, 16870–16875 (2006).
17. I. Appelmann *et al*., Janus kinase inhibition by ruxolitinib extends dasatinib- and dexamethasone-induced remissions in a mouse model of Ph+ ALL. *Blood* **125**, 1444–1451 (2015).
18. J. de Jong *et al*., The effect of food on the pharmacokinetics of oral ibrutinib in healthy participants and patients with chronic lymphocytic leukemia. *Cancer Chemother. Pharmacol.* **75**, 907–916 (2015).
19. M. R. Clark, S. A. Johnson, J. C. Cambier, Analysis of Ig-alpha-tyrosine kinase interaction reveals two levels of binding specificity and tyrosine phosphorylated Ig-alpha stimulation of Fyn activity. *EMBO J.* **13**, 1911–1919 (1994).
20. J. Zhang, P. L. Yang, N. S. Gray, Targeting cancer with small molecule kinase inhibitors. *Nat. Rev. Cancer* **9**, 28–39 (2009).
21. Y. Liu, K. Shah, F. Yang, L. Witucki, K. M. Shokat, A molecular gate which controls unnatural ATP analogue recognition by the tyrosine kinase v-Src. *Bioorg. Med. Chem.* **6**, 1219–1226 (1998).
22. M. Pfeifer *et al*., PTEN loss defines a PI3K/AKT pathway-dependent germinal center subtype of diffuse large B-cell lymphoma. *Proc. Natl. Acad. Sci. U.S.A.* **110**, 12420–12425 (2013).
23. J. J. Castillo, M. Furman, E. S. Winer, CAL-101: A phosphatidylinositol-3-kinase p110-delta inhibitor for the treatment of lymphoid malignancies. *Expert Opin. Investig. Drugs* **21**, 15–22 (2012).
24. I. W. Flinn *et al*., Duvelisib, a novel oral dual inhibitor of PI3K-δ,γ, is clinically active in advanced hematologic malignancies. *Blood* **131**, 877–887 (2018).
25. S. K. Pal, K. Reckamp, H. Yu, R. A. Figlin, Akt inhibitors in clinical development for the treatment of cancer. *Expert Opin. Investig. Drugs* **19**, 1355–1366 (2010).
26. B. Seto, Rapamycin and mTOR: A serendipitous discovery and implications for breast cancer. *Clin. Transl. Med.* **1**, 29 (2012).
27. S. V. Bhagwat *et al*., Preclinical characterization of OSI-027, a potent and selective inhibitor of mTORC1 and mTORC2: Distinct from rapamycin. *Mol. Cancer Ther.* **10**, 1394–1406 (2011).
28. M. R. Janes *et al*., Efficacy of the investigational mTOR kinase inhibitor MLN0128/INK128 in models of B-cell acute lymphoblastic leukemia. *Leukemia* **27**, 586–594 (2013).
29. E. K. Slotkin *et al*., MLN0128, an ATP-competitive mTOR kinase inhibitor with potent in vitro and in vivo antitumor activity, as potential therapy for bone and soft-tissue sarcoma. *Mol. Cancer Ther.* **14**, 395–406 (2015).
30. J. M. Umakanthan *et al*., Phase I/II study of dasatinib and exploratory genomic analysis in relapsed or refractory non-Hodgkin lymphoma. *Br. J. Haematol.* **184**, 744–752 (2019).
31. E. Battistello *et al*., Pan-SRC kinase inhibition blocks B-cell receptor oncogenic signaling in non-Hodgkin lymphoma. *Blood* **131**, 2345–2356 (2018).
32. M. S. Lionakis *et al*., Inhibition of B cell receptor signaling by ibrutinib in primary CNS lymphoma. *Cancer Cell* **31**, 833–843.e5 (2017).
33. K. Saijo *et al*., Essential role of Src-family protein tyrosine kinases in NF-kappaB activation during B cell development. *Nat. Immunol.* **4**, 274–279 (2003).
34. J. Paul *et al*., Simultaneous inhibition of PI3Kδ and PI3Kα induces ABC-DLBCL regression by blocking BCR-dependent and -independent activation of NF-κB and AKT. *Cancer Cell* **31**, 64–78 (2017).
35. N. Pallet, C. Legendre, Adverse events associated with mTOR inhibitors. *Expert Opin. Drug Saf.* **12**, 177–186 (2013).